TRIM50 Inhibits Gastric Cancer Progression by Regulating the Ubiquitination and Nuclear Translocation of JUP

Jiajia Hu, Runjie Huang, Chengcai Liang, Yingnan Wang, Min Wang, Yanxing Chen, Chenyi Wu, Jinling Zhang, Zekun Liu, Qi Zhao, Zexian Liu, Feng Wang, and Shuqiang Yuan

ABSTRACT

Gastric cancer is one of the most frequent cancers in the world. Emerging clinical data show that ubiquitination system disruptions are likely involved in carcinoma genesis and progression. However, the precise role of ubiquitin (Ub)-mediated control of oncogene products or tumor suppressors in gastric cancer is unknown. Tripartite motif-containing 50 (TRIM50), an E3 ligase, was discovered by high-output screening of ubiquitination-related genes in tissues from patients with gastric cancer to be among the ubiquitination-related enzymes whose expression was most downregulated in gastric cancer. With two different databases, we verified that TRIM50 expression was lower in tumor tissues relative to normal tissues. TRIM50 also suppressed gastric cancer cell growth and migration *in vitro* and *in vivo*. JUP, a transcription factor, was identified as a new TRIM50 ubiquitination target by MS and coimmunoprecipitation experiments. TRIM50 increases JUP K63-linked polyubiquitination mostly at the K57 site. We discovered that the K57 site is critical for JUP nuclear translocation by prediction with the iNuLoC website and further studies. Furthermore, ubiquitination of the K57 site limits JUP nuclear translocation, consequently inhibiting the MYC signaling pathway. These findings identify TRIM50 as a novel coordinator in gastric cancer cells, providing a potential target for the development of new gastric cancer treatment strategies.

Implications: TRIM50 regulates gastric cancer tumor progression, and these study suggest TRIM50 as a new cancer target.

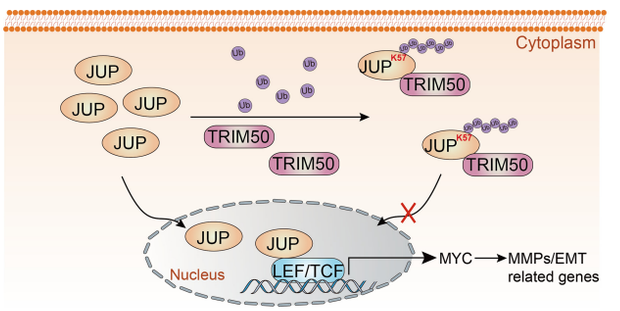

Introduction

Gastric cancer is a leading contributor to global cancer incidence and mortality. According to worldwide cancer data in 2020, more than 1 million new cases of gastric cancer were recorded that year, accounting for 5.6% of all cancers and ranking fifth. Approximately 770,000 fatalities were reported during 2020, accounting for 7.7% of all cancers and ranking fourth (1). The development of gastric cancer is related to many factors. For example, cardiac cancer is connected with obesity and gastroesophageal reflux disease (2). On the other hand, chronic *Helicobacter pylori* infection is the major cause of noncardiac cancer. Other contributing factors include smoking, drinking, excessive intake of pickled food, and insufficient intake of fruits and vegetables (3). In addition, psychologic stress factors and social support affect the quality of life of patients with gastric cancer, and more attention in clinical work is required (4). The incidence of gastric cancer is high in China, with approximately 43% of new cases and 48% of deaths occurring there (5). The onset of gastric cancer is insidious, with more than half of patients presenting with advanced-stage disease. Advanced gastric cancer has a poor prognosis. The overall survival of patients treated with conventional chemotherapy (e.g., platinum plus fluorouracil) does not exceed 1 year (6). Several biomarkers and targets, such as microsatellite instability status (MSI), programmed cell death ligand 1 (PD-L1), HER2, and tumor mutation burden (TMB), have been discovered to improve therapeutic effects (7). However, prognosis improvement is limited because of the complex pathogenesis of gastric cancer and heterogeneity between individuals (8). The need to investigate the mechanisms underlying gastric cancer progression for novel therapeutic strategies is urgent.

Ubiquitination, an important posttranslational modification, is a process by which ubiquitin (Ub, a small and highly conserved protein) classifies proteins by target protein selection and modification with assistance from a series of special enzymes (9). The general ubiquitination process requires three kinds of enzymes. E1 enzymes activate the Ub polypeptide. Then, activated Ub polypeptides are conjugated to E2 enzymes via thioester bonds. Finally, E3 Ub ligases recognize both E2 enzymes and specific target substrates and transfer Ub from E2 enzymes to target substrates (10). Ubiquitination is essential

State Key Laboratory of Oncology in South China, Collaborative Innovation Center for Cancer Medicine, Sun Yat-sen University Cancer Center, Sun Yat-sen University, Guangzhou, P.R. China.

J. Hu, R. Huang, and C. Liang contributed equally to this article.

Corresponding Authors: Shuqiang Yuan, Department of Gastric Surgery, Sun Yat-sen University Cancer Center, Yuexiu, Guangzhou, Guangdong, 510060, China. E-mail: yuanshq@sysucc.org.cn.or; and Feng Wang, wangfeng@sysucc.org.cn

Mol Cancer Res 2023;21:1107–19

doi: 10.1158/1541-7786.MCR-23-0113

for various cellular processes, including division, migration, differentiation, and fate specification (11–14). Emerging evidence suggests that ubiquitination is dysregulated in human cancer (15). For example, the deubiquitination enzyme OTUB1 controls the stability of the GPX4 protein, thus promoting gastric cancer dissemination (16). Abolishing the classical deubiquitination enzyme USP7 reduced PD-L1 expression and made gastric cancer cells more susceptible to cytocytoxic T cells (17). Thus, a current focus of cancer research is the identification and targeting of E3 ligases involved in the regulation of oncoproteins and tumor-suppressor proteins. However, the underlying mechanism by which ubiquitination controls oncogene products or tumor suppressors in gastric cancer still needs further investigation. Tripartite motif-containing protein 50 (TRIM50) is a member of the tripartite motif (TRIM) protein family, one of the largest subfamilies of E3 ligases (18). TRIM50 has been shown to act as a tumor suppressor in hepatocellular carcinoma, ovarian cancer, and pancreatic cancer (19–21). In gastric tissue, TRIM50 was reported to promote the formation of sophisticated canaliculi and microvilli during acid secretion from parietal cells (22). However, the role of TRIM50 in gastric cancer is not clear.

In our study, we analyzed the expression of TRIM50 in gastric cancer and explored the roles of TRIM50 in gastric cancer progression. TRIM50 inhibited gastric cancer cell proliferation and migration *in vitro* and repressed gastric cancer growth and dissemination *in vivo*. Mechanistically, TRIM50 inhibited the MYC signaling pathway by targeting JUP and promoting its K63-linked ubiquitination at the site K57, thus inhibiting JUP nuclear translocation.

Materials and Methods

Cell lines and gastric cancer tissues

The human gastric cancer cell lines MKN7, MKN74, AGS, MKN45, SNU-668, and HGC27 were purchased from ATCC. The cells were cultured in RPMI1640 medium (HyClone) or DMEM (HyClone) medium with 10% FBS and antibiotics (100 μg/mL penicillin and 100 μg/mL streptomycin) at 37°C in a 5% CO_2 cell culture incubator, as recommend by ATCC. Mycoplasma testing was conducted with Mycoplasma Detector (Vazyme, D101–02) every 2 weeks to ensure that mycoplasma-negative and all cells were not used after more than 10 passages. All cell lines were authenticated by STR fingerprinting at the Medicine Lab of the Forensic Medicine Department of Sun Yat-sen University before use. Data from a cohort of patients with gastric cancer ($n = 159$) who underwent gastrectomy at Sun Yat-sen University Cancer Center (SYSUCC) between 2007 and 2009 were retrieved. mRNA samples of tumor tissues had been obtained from all patients, and mRNA samples of adjacent normal tissues were available from 123 of 159 patients. In addition to these samples, we collected 39 paired mRNA and paraffin-embedded samples from both tumor tissues and adjacent normal tissues from patients who received gastrectomy at SYSUCC in 2010. Written informed consent was obtained from each participant, and the study was authorized by the Institutional Review Board of the Sun Yat-sen University Cancer Center in accordance with the Declaration of Helsinki.

Plasmid and lentivirus transfection

TRIM50 overexpression and knockdown lentiviruses were synthesized by OBiO Technology Corp., Ltd. Cells were transfected with lentiviruses in the presence of 5 μg/mL polybrene for 72 hours, and then GFP-positive cells were selected by flow cytometry. The wild-type TRIM50 overexpression plasmid was constructed by Tsingke Bio Co., Ltd. Domain deletion mutant TRIM50 plasmids were subcloned using the wild-type plasmid as a template. The efficiency of shRNA transfection was measured at 48 hours post-transfection by Western blotting. The shRNA sequences used were as follows:

*TRIM50*_sh1: GGCTCTACCTGCACTATGA
*TRIM50*_sh2: TCGCCAAACTGGTGAACAA.

Colony formation assay

For the colony formation assay, cells were seeded at a density of 500 cells/well in 6-well plates with 10% FBS-containing culture medium. The medium was replaced every 3 days. After 15 days, the colonies were fixed with methanol and stained with 0.1% crystal violet (Sigma-Aldrich). Colony formation was determined by counting the number of stained colonies.

Cell proliferation assay

The cells were seeded in 96-well plates at a density of 1×10^3 cells/well. At the time points indicated in the figures, 20 μL of MTT dye was added to the wells and incubated for 4 hours at 37°C. The spectrometric absorbance at a wavelength of 490 nm was determined by a microplate reader (Tecan). Each sample had four replicates.

Wound healing assay

The cells were incubated in 6-well plates at a density of 1×10^6 cells/well and allowed to reach 100% confluence. The cell monolayer was wounded by dragging a 200-μL pipette tip. The cells were washed to remove cellular debris and then allowed to migrate for 48 hours. Images were captured at 0 and 48 hours after wounding under an inverted microscope.

Transwell migration assay

Transwell migration assays were performed in 24-well plates with 8-μmol/L pore-sized Transwells in accordance with the manufacturer's instructions. The lower chamber was filled with culture medium supplemented with 30% FBS, whereas the upper chamber was filled with 5×10^4 cells in culture medium without FBS. After incubation for 48 hours at 37°C, the cells on the lower surface of the membrane were dyed with crystal violet and counted by a technician blinded to the experimental settings in four randomly selected microscopic fields of each filter. The tests were repeated three times.

RT-qPCR

Total RNA was extracted using TRizol reagent (Thermo Fisher Scientific, 15596026) and reverse transcribed into cDNA with HiScript II Q RT SuperMix for qPCR (Takara, RR036Q). Then, the mRNA levels of the target genes were quantified by qPCR using 2× RealStar Green Power Mixture (Promega, A6002). All the data were normalized to the input. The primers were synthesized by Tsingke Bio Co., Ltd. The sequences are listed in Supplementary Table S1.

IP and IP MS

For immunoprecipitation (IP) assays, whole-cell extracts were prepared after Flag-TRIM50 transfection, which was followed by incubation overnight with the appropriate antibodies plus Protein A/G beads (Pierce, 20,423). For IP with anti-Flag, anti-Flag agarose gels (Sigma, A2220) were used. Immunocomplexes were then washed five times with RIPA buffer (Beyotime, P0013B). Then, the immunoprecipitates were eluted with 1× SDS loading buffer (Beyotime, P0015). Cell lysates were separated by electrophoresis with a 10% SDS-PAGE gel. For co-IP assays, the proteins were transferred to PVDF membranes (Bio-Rad) and further subjected to Western blot analysis. For IP mass spectrometry, the gel

was stained with Coomassie (Beyotime, ST030), and the target strip was cut away and sent for MS (APTBIO; ref. 23).

Western blot analysis

Total cell proteins were obtained using RIPA buffer, and nuclear/cytoplasmic separation proteins were obtained using a Protein Extraction Kit (Beyotime, P0027) following the manufacturer's instructions. Cell lysates were separated by electrophoresis with a 10% SDS-PAGE gel, after which the proteins were transferred to PVDF membranes (Bio-Rad, 1,620,177) and further incubated with the appropriate antibodies. Horseradish peroxidase (HRP)-conjugated anti-mouse or anti-rabbit IgG was used as the secondary antibody as appropriate. The protein bands were visualized and visualized using an enhanced chemiluminescence system (Tanon, 180–501). The antibodies used in this study were as follows: anti-CDH2 (ab5451), anti-Vimentin (ab137321), anti-Slug (ab183760), anti-JUP (ab251317), anti-Lamin B1 (ab16048), and anti-β-Tubulin (ab15568) purchased from Abcam; goat anti-rabbit IgG-HRP (RS0002), goat anti-mouse IgG-HRP (RS0007), and anti-GAPDH (YM3215) purchased from ImmunoWay (Immunoway); anti-TRIM50 (HPA019862), HRP-anti-Flag (M2) (A8592), and anti-β-Actin (A1978) purchased from Sigma; and anti-HA-HRP (11667475001) purchased from Roche Applied Science.

In vivo tumorigenesis and dissemination models

For tumorigenesis experiments, 4- to 6-week-old female BALB/c nude mice (Beijing Vital River Laboratory Animal Technology Co., Ltd.) were used. Randomization was conducted, and the mice were treated in an unblinded manner. The solution used for cell suspension was a mixture of Matrigel (Corning, 354248) and PBS (GIBCO, C10010500CP) at a 1:1 ratio. Cells (5×10^6 MKN45 cells or 1×10^7 MKN74 cells suspended in 100-μL solutions) were subcutaneously injected into the flank of the mice. Tumor size was measured every three days with a caliper, and tumor volume was determined with the standard formula $V = {}^1/_2$ (length $\times$ width^2). At the end stage, tumor weight was measured. For dissemination experiments, two xenograft models were established as described in a previous study (24). For the peritoneal tumor dissemination model, TRIM50-overexpressing MKN45 cells were labeled with luciferase and directly injected into the peritoneum. Dissemination was evaluated by bioluminescent imaging for 8 weeks. Then, the mice were euthanized, and the nodules in the peritoneum were counted. For the tail vein injection dissemination model, cells were injected into the median tail vein. Distant dissemination was monitored by bioluminescent imaging. The mice were euthanized in the 10th week, and then the lungs were embedded in paraffin and stained with hematoxylin and eosin (H&E). In the bioluminescence imaging experiment, we set a threshold for bioluminescence to ensure that bioluminescence from the same set of experiments can be compared. All animal experiments were performed in accordance with protocols approved by the Institutional Animal Care Committee.

Statistical analysis

Data and error bars represent the mean ± SD of at least three independent experiments. Sample size determination was based on the need for statistical power. Experiments with patient samples were performed in a blinded manner. Two-tailed Student *t* test was used to analyze the differences between groups. All analyses were carried out using GraphPad Prism version 8.0.2 (GraphPad Software). When $P < 0.05$, the results were considered statistically significant.

Results

TRIM50 was downregulated in gastric cancer tissues compared with adjacent normal tissues

First, we screened 310 differentially expressed genes (DEG) in 300 gastric cancer tissues compared with 98 normal gastric tissues from the GSE66229 dataset using the indicated fold change (FC) ratio ($|\log_2 FC| > 2$) and adjusted *P* value (P value < 0.05). Then, we overlapped these 310 DEGs with 814 human ubiquitination-related genes from the Gene Ontology (GO) database. Eight intersecting genes were obtained (**Fig. 1A**). Among these 8 genes, TRIM50 was downregulated to the greatest extent, and its downregulation was specific to gastric cancer in The Cancer Genome Atlas (TCGA) database (**Fig. 1B**; Supplementary Fig. S1A; Supplementary Information). To confirm these results, we collected 39 paired gastric cancer tumor tissues and adjacent normal tissues. By analyzing the RNA expression levels by RT-qPCR, we found that the expression levels of TRIM50 were significantly lower in gastric cancer tissues compared with paired normal tissues, which was consistent with the RNA sequencing data in the GSE66229 dataset (**Fig. 1C**). We next verified the mRNA expression levels of TRIM50 in a larger gastric cancer cohort from our center by RT-qPCR and TCGA database. The expression levels of TRIM50 were significantly lower in gastric cancer tumor tissues than in adjacent normal tissues (**Fig. 1D**). Furthermore, we compared TRIM50 protein levels between tumor and normal tissues in the EOGC Data Portal. As expected, TRIM50 showed lower protein expression levels in gastric cancer tumor tissues (**Fig. 1E**). To further confirm the protein expression pattern of TRIM50, we performed IHC staining of five paired gastric cancer tissues and adjacent normal tissues from SYSUCC patients with gastric cancer. The results showed that TRIM50 expression was significantly downregulated in gastric cancer tumor tissues compared with normal tissues (**Fig. 1F**; Supplementary Fig. S1B; Supplementary Information). Moreover, immunoblotting showed the same change in TRIM50 expression levels (**Fig. 1G**). These results suggest that TRIM50 is downregulated in gastric cancer tissues compared with adjacent normal tissues and that this downregulation may affect gastric cancer progression.

TRIM50 suppressed gastric cancer cell proliferation and migration *in vitro*

To investigate the roles of TRIM50 in gastric cancer progression, we first detected the expression levels of TRIM50 in different gastric cancer cell lines by immunoblotting assay (Supplementary Fig. S2; Supplementary Information). TRIM50 was highly expressed in SNU-668 cells and expressed at low levels in MKN45 cells. To develop *TRIM50*-knockdown cells, we transfected SNU-668 cells with lentiviruses containing *TRIM50* shRNA. The *TRIM50* knockdown efficiency was confirmed by immunoblotting assay (**Fig. 2A**). To verify the functions of TRIM50 in SNU-668 cells, we first determined the proliferation of *TRIM50*-knockdown gastric cancer cells. MTT assays and colony formation assays showed that *TRIM50* knockdown accelerated gastric cancer cell growth (**Fig. 2B** and **C**). In addition, cell migration assays and wound healing assays showed that *TRIM50* knockdown enhanced the migration of gastric cancer cells (**Fig. 2D** and **E**). To further evaluate the roles of TRIM50, MKN45 cells with stable TRIM50 expression were established with lentivirus expressing Flag-TRIM50, and the expression of TRIM50 in these cells was confirmed by immunoblotting (**Fig. 2F**). Then, we compared the cell proliferation rates of TRIM50-overexpressing and control (EV) gastric cancer cells by using MTT assays. Cells with TRIM50 overexpression had a lower proliferation rate than those in the EV group (**Fig. 2G**).

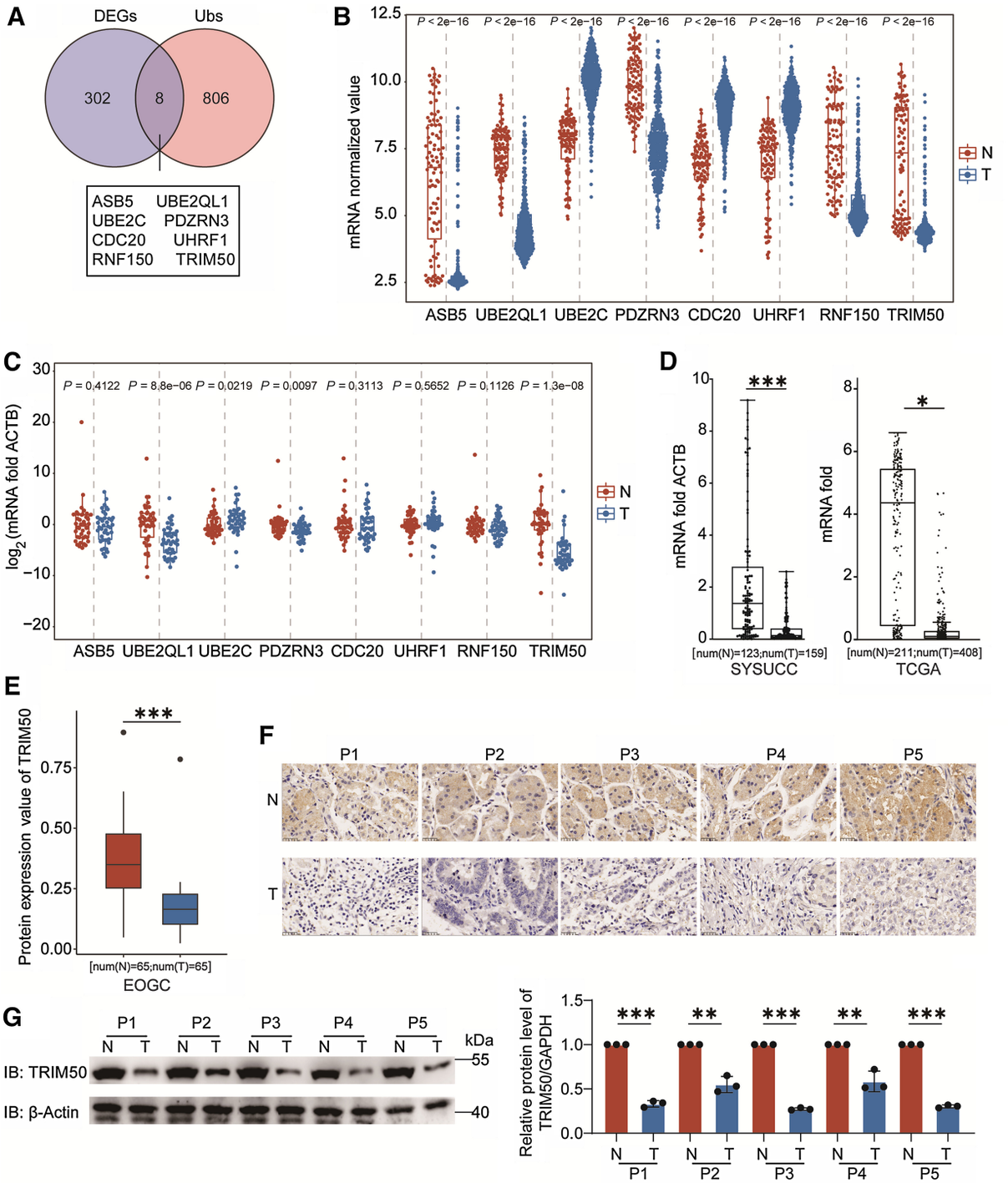

Figure 1.

TRIM50 was expressed at lower levels in gastric cancer tumor tissues compared with normal gastric tissues. **A,** Overlap of 310 DEGs (GSE66229 database) with a list of 814 human ubiquitination-related genes (GO database). **B,** The mRNA expression of 8 genes screened from (A) gastric cancer tumor tissues (T) and adjacent normal tissues (N) in the GSE66229 dataset is shown. **C,** RT-qPCR analysis of the mRNA expression of 8 genes screened from (**A**) in 39 paired gastric cancer tumor tissues and adjacent normal tissues from SYSUCC patients with gastric cancer. ACTB was used as a control. **D,** Left, RT-qPCR analysis of TRIM50 mRNA expression in tumor tissues and adjacent normal tissues from SYSUCC patients with GC. Right, the mRNA levels of TRIM50 in The Cancer Genome Atlas (TCGA) database. **E,** Analysis of TRIM50 protein expression in tumor tissues and adjacent normal tissues from EOGC. **F,** Representative IHC images of TRIM50 expression in five paired gastric cancer tumor tissues and paired adjacent normal tissues from SYSUCC patients with gastric cancer. Scale bar: 25 μm. **G,** TRIM50 protein levels in five paired gastric cancer tumor tissues and adjacent normal tissues from SYSUCC patients with gastric cancer determined by immunoblotting assay.

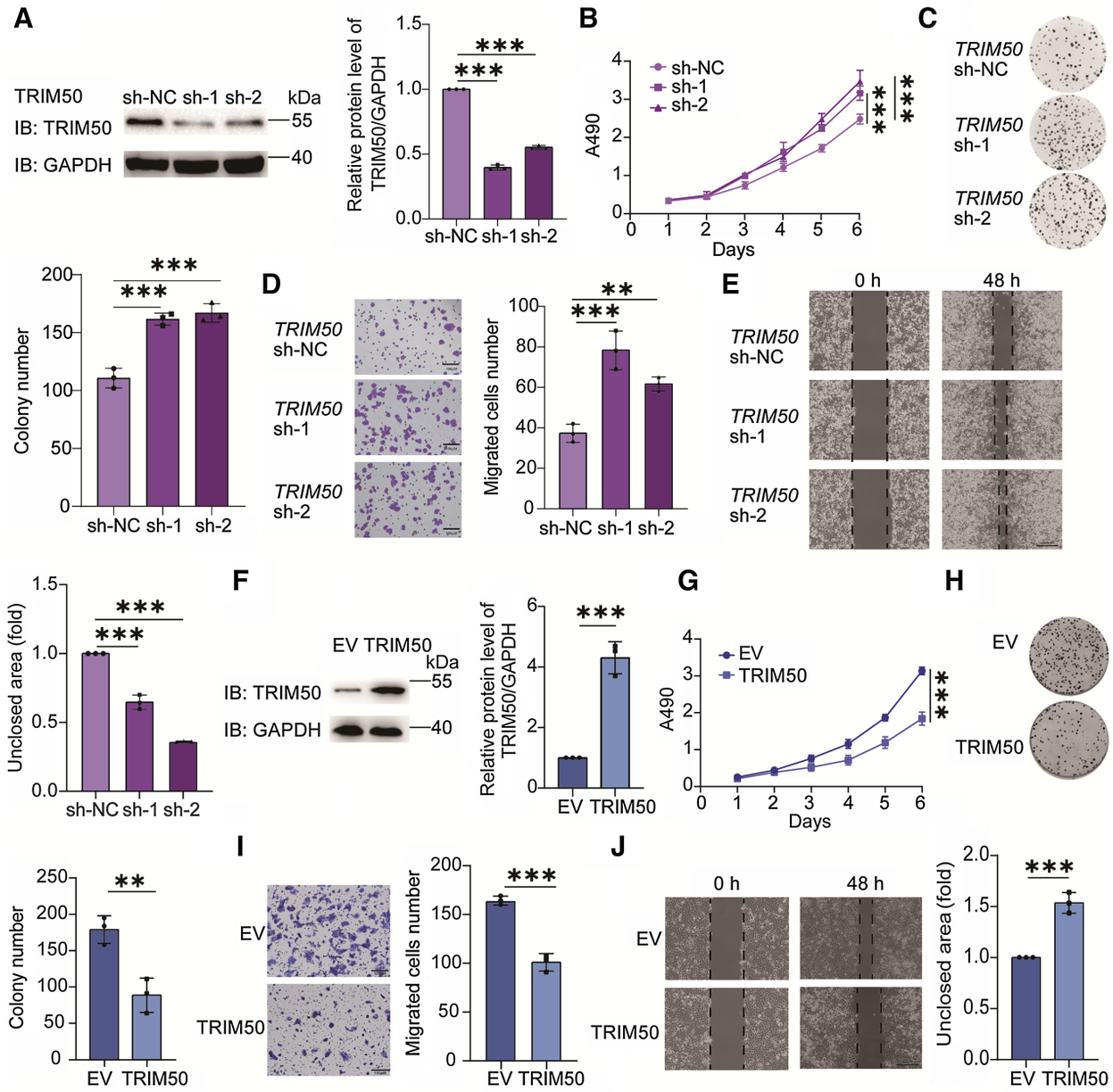

Figure 2.

TRIM50 suppressed gastric cancer cell proliferation and migration *in vitro*. **A,** SNU-668 cells were transfected with lentiviruses expressing *TRIM50* shRNA. A universal nonsilencing shRNA was used as a negative control (sh-NC). Whole-cell lysates were subjected to immunoblot analysis with TRIM50 antibody. **B,** The proliferation of *TRIM50*-knockdown SNU-668 cells was estimated using the MTT assay. **C,** The colony formation capacity of *TRIM50*-knockdown SNU-668 cells was determined by counting the colonies. **D,** Images and quantification of data from Transwell migration assays of *TRIM50*-knockdown SNU-668 cells. Scale bar, 100 μm. **E,** Wound healing in *TRIM50*-knockdown SNU-668 cells was recorded and quantitatively analyzed. Scale bar, 200 μm. **F,** Immunoblotting of empty vector (EV) versus TRIM50-overexpressing (TRIM50) MKN45 cells and quantitative analysis. MKN45 cells were infected with lentivirus expressing TRIM50. An EV was used as a control. **G,** The proliferation of TRIM50-overexpressing MKN45 cells was estimated using the MTT assay. **H,** Colony assays with TRIM50-overexpressing MKN45 cells. **I,** Images and quantification following Transwell migration assays with TRIM50-overexpressing MKN45 cells. Scale bar, 100 μm. **J,** Wound healing assays with TRIM50-overexpressing MKN45 cells. Scale bar, 200 μm.

Cell colony formation assays showed that the TRIM50 overexpression group formed fewer colonies than the EV group (**Fig. 2H**). In addition, overexpression of TRIM50 significantly decreased cell migration compared with that in the control group (**Fig. 2I** and **J**). Taken together, our data indicated that TRIM50 suppressed gastric cancer cell proliferation and migration *in vitro*.

TRIM50 restrained tumor growth and dissemination *in vivo*

To evaluate the functions of TRIM50 *in vivo*, we used a nude mouse subcutaneous xenograft model. Compared with EV gastric cancer cells, the use of gastric cancer cells overexpressing TRIM50 led to a significantly lower tumor growth rate and tumor weight (**Fig. 3A** and **B**; Supplementary Fig. S3A, Supplementary Information).

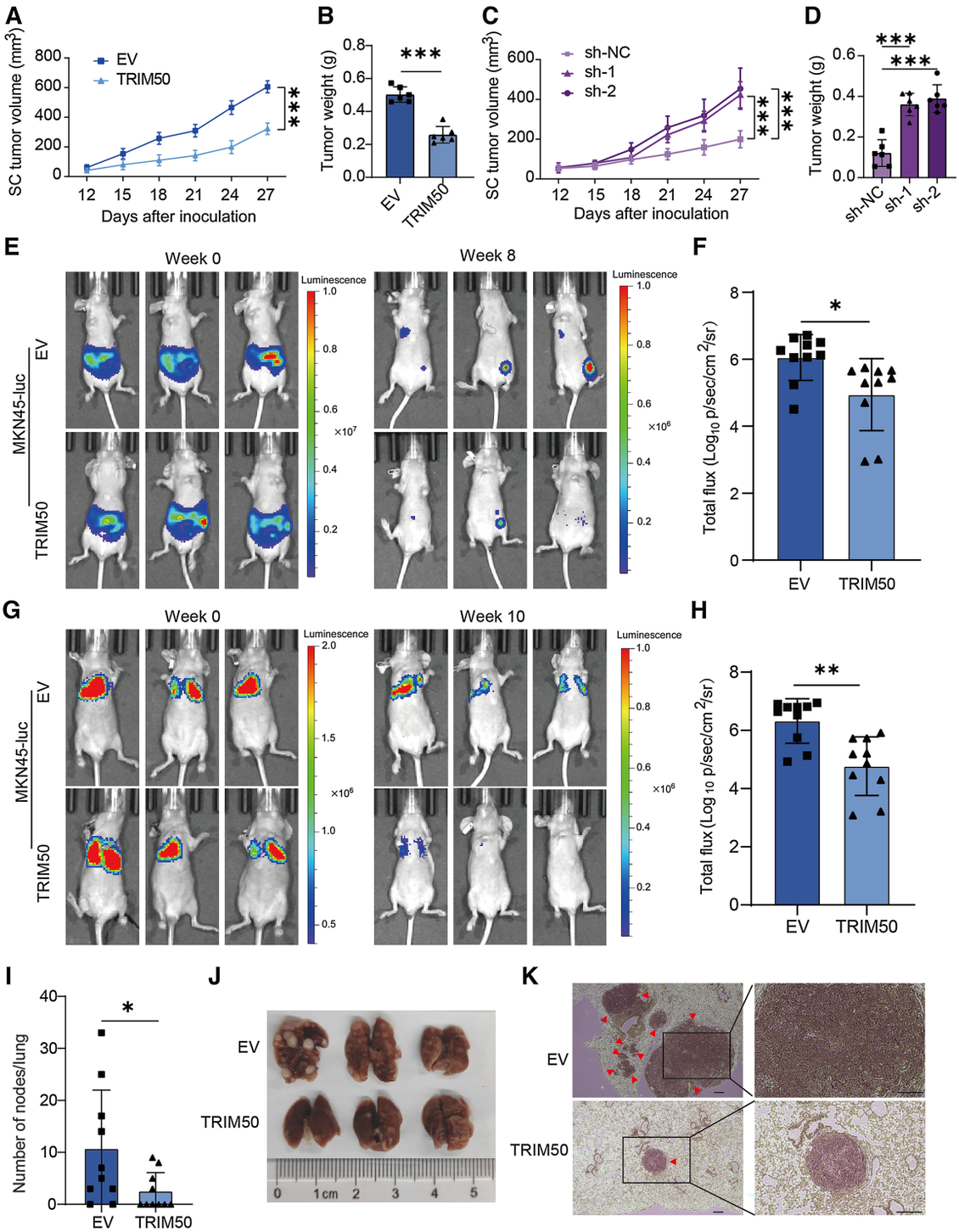

Figure 3.

TRIM50 restrained tumor growth and dissemination *in vivo*. **A** and **B,** Tumor growth rate (**A**) and quantification of excised subcutaneous tumors (**B**) in a nude mouse subcutaneous xenograft model in which TRIM50-overexpressing (TRIM50) versus control empty vector (EV) MKN45 cells were implanted ($n = 6$ mice per group). Scale bar: 1 cm. **C** and **D,** Tumor growth rate (**C**) and quantification of excised subcutaneous tumors (**D**) in a nude mouse subcutaneous xenograft model in which *TRIM50*-knockdown MKN74 cells were implanted ($n = 6$ mice per group). Scale bar, 1 cm. **E,** Representative bioluminescent imaging of a nude mouse peritoneal dissemination tumor model prepared with TRIM50-overexpressing MKN45-luc cells at week 0 and week 8 ($n = 10$ mice per group). **F,** The bioluminescence of peritoneal dissemination nodes in the TRIM50 and EV groups was quantified and analyzed. **G,** Representative bioluminescent imaging of the nude mouse tail vein injection model prepared with TRIM50-overexpressing MKN45-luc cells at week 0 and week 10 ($n = 10$ mice per group). **H,** The bioluminescence of the lung nodes was quantified and analyzed. **I,** The numbers of lung nodes in the TRIM50 and EV groups were analyzed. **J** and **K,** Representative specimens (**J**) and hematoxylin and eosin (H&E) staining photographs (**K**) of the nodes from the lungs of the TRIM50 and EV groups. Scale bar, 200 μm.

Furthermore, *TRIM50* knockdown slowed tumor growth *in vivo* (**Fig. 3C** and **D**; Supplementary Fig. S3B; Supplementary Information). We further investigated the effects of TRIM50 overexpression on tumor dissemination *in vivo* with two models prepared with luciferase-labeled gastric cancer cells, a peritoneal dissemination model and tail vein dissemination model. In the peritoneal dissemination model, TRIM50 overexpression decreased peritoneal dissemination in mice bearing MKN45 cells (**Fig. 3E** and **F**). Similarly, in the tail vein model, TRIM50 overexpression led to a lower bioluminescence intensity than that in the control group (**Fig. 3G** and **H**). Moreover, overexpression of TRIM50 decreased the number of disseminated nodes in the lung (**Fig. 3I–K**). Altogether, our data revealed that TRIM50 decreased tumor growth and dissemination potential *in vivo*.

TRIM50 inhibits the MYC signaling pathway

Subsequently, we sought to explore the signaling pathway that is affected by the role of TRIM50 in regulating gastric cancer progression. We performed RNA sequencing analysis of TRIM50-overexpressing MKN45 cells. Gene set enrichment analysis (GSEA) indicated significant enrichment of the MYC target V2 and MYC target V1 gene sets in TRIM50-overexpressing cells (**Fig. 4A** and **B**). We next examined MYC mRNA expression levels in TRIM50-overexpressing MKN45 cells. RT-qPCR analysis showed that *MYC* expression was decreased in TRIM50-overexpressing cells compared with control cells (**Fig. 4C**). Consistently, the mRNA expression levels of MYC target genes, such as *MMP13, CDH2, Vimentin,* and *Slug* (25), were decreased in TRIM50-overexpressing cells compared with control cells (**Fig. 4D**). Immunoblotting analysis confirmed that TRIM50 upregulation attenuated the protein levels of CDH2, Vimentin, and Slug in gastric cancer cells (**Fig. 4E**). To further explore whether the role of TRIM50 depends on MYC, we overexpressed TRIM50 with or without c-myc in MKN45 cells. MTT and Transwell assays showed that TRIM50-mediated cell proliferation and migration repression was weakened with c-myc overexpression in MKN45 cells (**Fig. 4F** and **G**). In brief, our findings showed that TRIM50 inhibits the MYC signaling pathway in gastric cancer cells. Thus, these data indicated that TRIM50 suppresses gastric cancer cell proliferation and migration via the MYC signaling pathway.

JUP is a binding target of TRIM50

To further define the target molecule of TRIM50, we conducted MS and co-IP assays to identify potential substrates of TRIM50 (**Fig. 5A**). Among the identified proteins, JUP, which was reported to directly activate MYC transcription, ranked first behind TRIM50 (26–28). Our results also showed that JUP overexpression activated *MYC* transcription, which indicated that JUP might interact with TRIM50 (**Fig. 5B** and **C**). In fact, co-IP assays confirmed that TRIM50 interacts with JUP (**Fig. 5D** and **E**). The TRIM50 structure consists of four domains: a RING-finger domain, a B-box domain, a C–C domain, and a PRY-SPRY domain (29). We next determined which domain of TRIM50 is involved in the interaction between TRIM50 and JUP using I-TASSER-MTD, a deep-learning-based platform for multidomain protein structure and function prediction (30). The results showed that TRIM50 might bind JUP via the RING-finger domain and the PRY-SPRY domain (Supplementary Fig. S4; Supplementary Information). Next, we constructed four TRIM50 truncation mutants in which the RING-finger domain, B-box domain, coiled-coil (CC) domain, or PRY-SPRY domain was deleted (**Fig. 5F**). IP showed that the construct lacking the PRY-SPRY domain interacted more weakly with JUP than the other constructs (**Fig. 5G** and **H**). Thus, these data indicated that TRIM50 interacts with JUP through its SPRY domain. In brief, our findings showed that JUP is a binding target of TRIM50 in gastric cancer cells.

TRIM50 stimulates the K63-linked polyubiquitination of JUP

As an E3 Ub ligase, we speculated that TRIM50 exerts its E3 ligase activity against JUP. Thus, we used an IP assay to verify whether TRIM50 could add a polyubiquitin chain to JUP. As expected, our data showed that the overexpression of TRIM50 enhanced the polyubiquitination of JUP (Supplementary Fig. S5; Supplementary Information). To further verify the involvement of TRIM50 in the ubiquitination of JUP, we performed an endogenous ubiquitination assay in MKN45 cells with stable TRIM50 expression and *TRIM50*-knockdown SNU-668 cells. Co-IP assays showed that TRIM50 overexpression significantly increased ubiquitination of the JUP protein (**Fig. 6A**). In contrast, *TRIM50* knockdown led to a reduction in the ubiquitination of JUP in SNU-668 cells (**Fig. 6B**). Furthermore, the TRIM50 △R failed to enhance the ubiquitination of JUP in 293T cells (**Fig. 6C**). To identify the Ub-binding sites of JUP, we used UbPred software to perform an *in silico* search and discovered several conserved sites in JUP, including K12, K57, K124, and K149. Next, we created JUP mutants in which each putative ubiquitination site was changed from lysine (K) to arginine (R). Among the mutants, JUP K57R showed a decrease in ubiquitination compared with that with the WT (**Fig. 6D**). There are eight different types of polyubiquitylation: Lys6, Lys11, Lys27, Lys29, Lys33, Lys48, and Lys63, and Met1-linked or "linear" chains (31). Lys48-linked chains are the most common chains in cells, and they function to direct proteins to the proteasome for degradation (32). In contrast, the second most prevalent chain type, connection via Lys63, serves a variety of nondegradative functions, including protein kinase activation, membrane trafficking, and DNA repair (33). Next, we examined the linkage types of Ub chains on JUP mediated by TRIM50 by using different mutants of Ub. We found that TRIM50 could specifically enhance the K63-linked ubiquitination of JUP and displayed low preference for other types of Ub linkages on JUP (**Fig. 6E**). Altogether, our results indicated that TRIM50 promotes the K63-linked polyubiquitination of JUP in a manner dependent on the RING domain.

TRIM50 regulates JUP nuclear transport in an Ub-dependent manner

Polyubiquitin chain linking is thought to be important for determining the effects of ubiquitylation. K48-, K11-, and K29-linked polyubiquitylation has been linked to proteasomal degradation, whereas the K63-linkage is involved in the regulation of numerous nonproteasomal pathways, such as protein kinase activation, membrane trafficking and DNA repair (34). To further define whether TRIM50 influences the expression of JUP, we detected JUP protein levels in TRIM50-overexpressing cells by western blotting. Our data verified that TRIM50 did not significantly change JUP expression at the protein level (Supplementary Fig. S6). A previous study reported that the JUP subcellular distribution is linked to gastric cancer formation and tumor differentiation status. Nuclear JUP was reported to interact with β-catenin and TCF4 and play a synergistic role with β-catenin to fuel gastric cancer cell invasion, whereas cytoplasmic JUP has the opposite effect (35). We therefore investigated whether TRIM50 regulates JUP nuclear translocation activity. A TRIM50 overexpression assay showed that more cytoplasmic JUP accumulated upon TRIM50 overexpression than in the control group of MKN45 cells (**Fig. 7A**). To gain insight into the underlying mechanism, we predicted the JUP nuclear localization sequence with the iNuLoC webserver and found that the K57 ubiquitination site is in

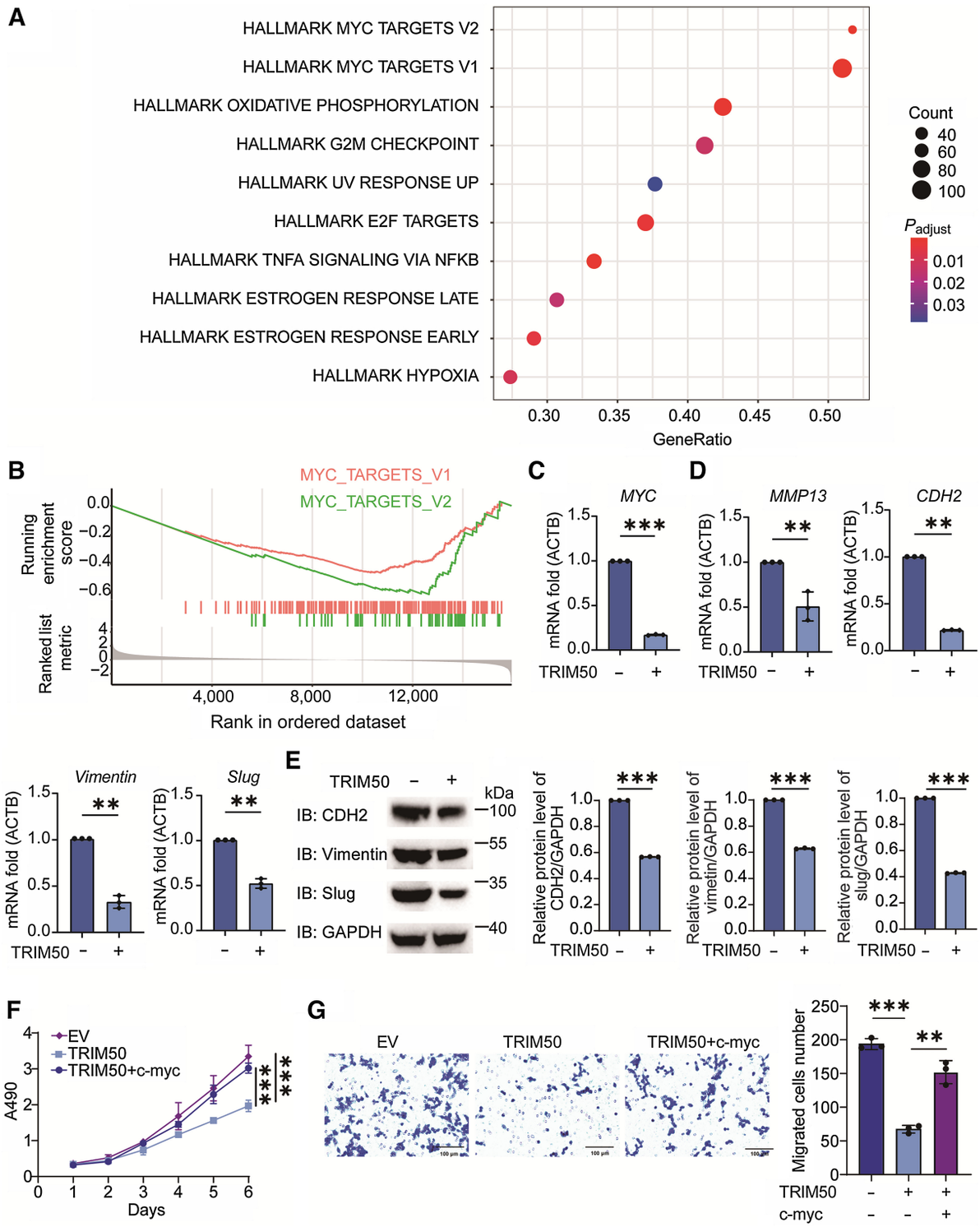

Figure 4.

TRIM50 inhibits the MYC signaling pathway. **A,** Results of HALLMARK signaling pathway enrichment analysis. The size of the dots represents the number of genes in different HALLMARK pathways, and the colors of the dots indicate the change in the adjusted *P* value. **B,** Representative GSEA plots were enriched in the MYC target V2 and MYC target V1 signaling pathway gene sets upon TRIM50 overexpression. **C,** RT-qPCR analysis of MYC in TRIM50-overexpressing (TRIM50) versus control empty vector (EV) MKN45 cells. **D,** RT-qPCR analysis of MMP13, CDH2, Vimentin, and Slug in TRIM50-overexpressing versus control EV MKN45 cells. **E,** Immunoblotting analysis of CDH2, Vimentin and Slug in TRIM50-overexpressing versus control EV MKN45 cells and quantitative analysis. **F,** The proliferation of TRIM50-overexpressing cells with or without c-myc versus control MKN45 cells was estimated using the MTT assay. **G,** Images and quantification of Transwell migration assays with TRIM50-overexpressing cells with or without c-myc versus control MKN45 cells. Scale bar, 100 μm.

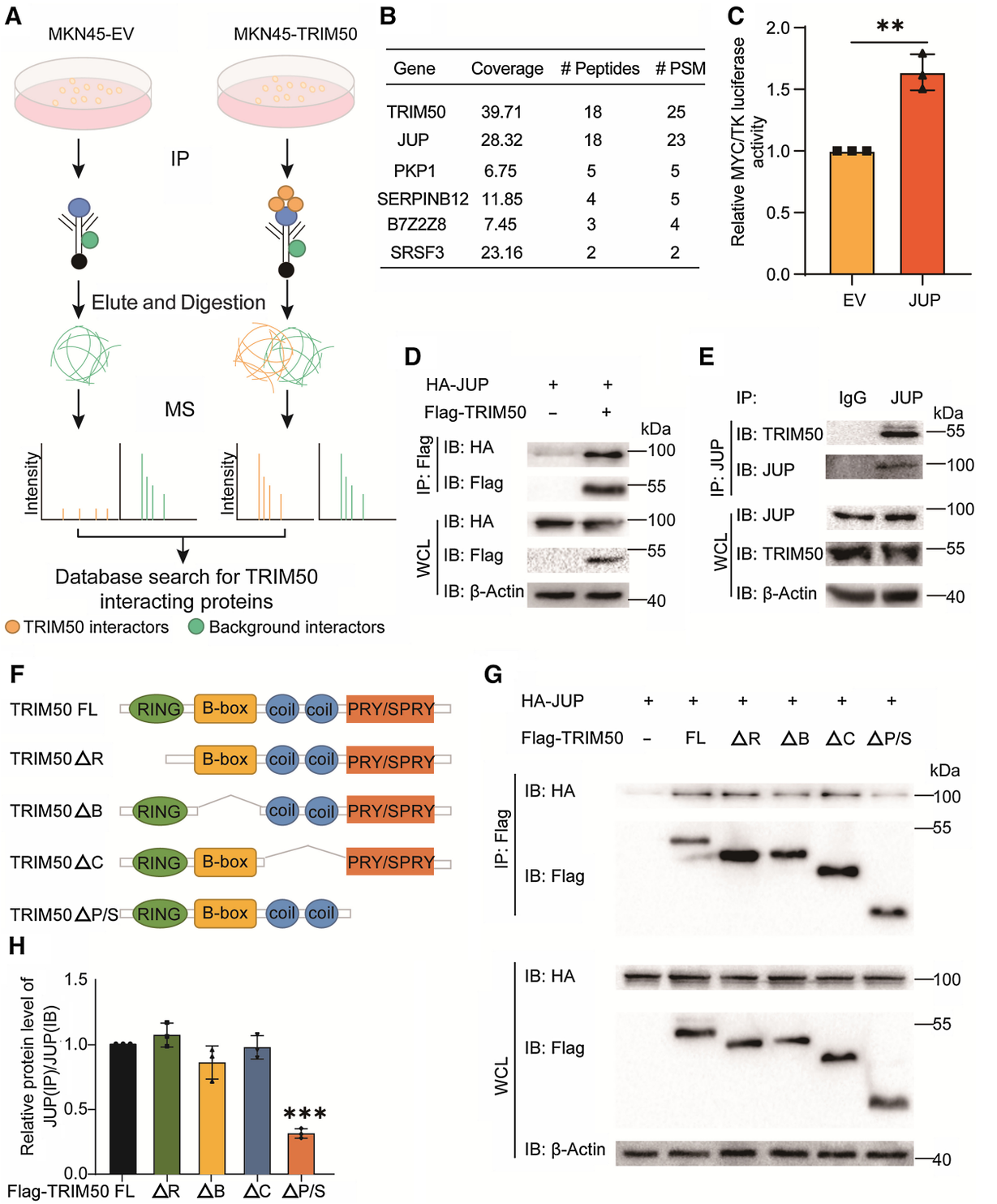

Figure 5.

JUP is a binding target of TRIM50. **A,** Flow chart for IP-MS. **B,** The genes with top coverage identified by IP-MS. **C,** 293T cells were transfected with plasmids encoding HA-JUP and MYC-luc/TK-luc. Cell lysates were subjected to MYC-luciferase reporter assays. **D,** 293T cells were transfected with plasmids encoding either Flag-TRIM50 or HA-JUP alone or in combination. Cell lysates were immunoprecipitated with Flag beads, and immunoblotting was performed with the indicated antibodies. **E,** SNU-668 cell lysates were subjected to SDS denaturation and immunoprecipitation with JUP antibody and immunoblot analysis with the indicated antibodies. **F,** The schematic diagram shows the structural domains of TRIM50 and the construction of the deletion constructs. **G** and **H,** 293T cells were transfected with HA-JUP along with Flag-empty vector (EV), Flag-TRIM50 full length (FL), ΔR, ΔB, ΔC, and ΔS. Whole-cell lysates were subjected to IP with anti-Flag beads. Immunoblot analysis was performed with the indicated antibodies, and the data were quantitatively analyzed.

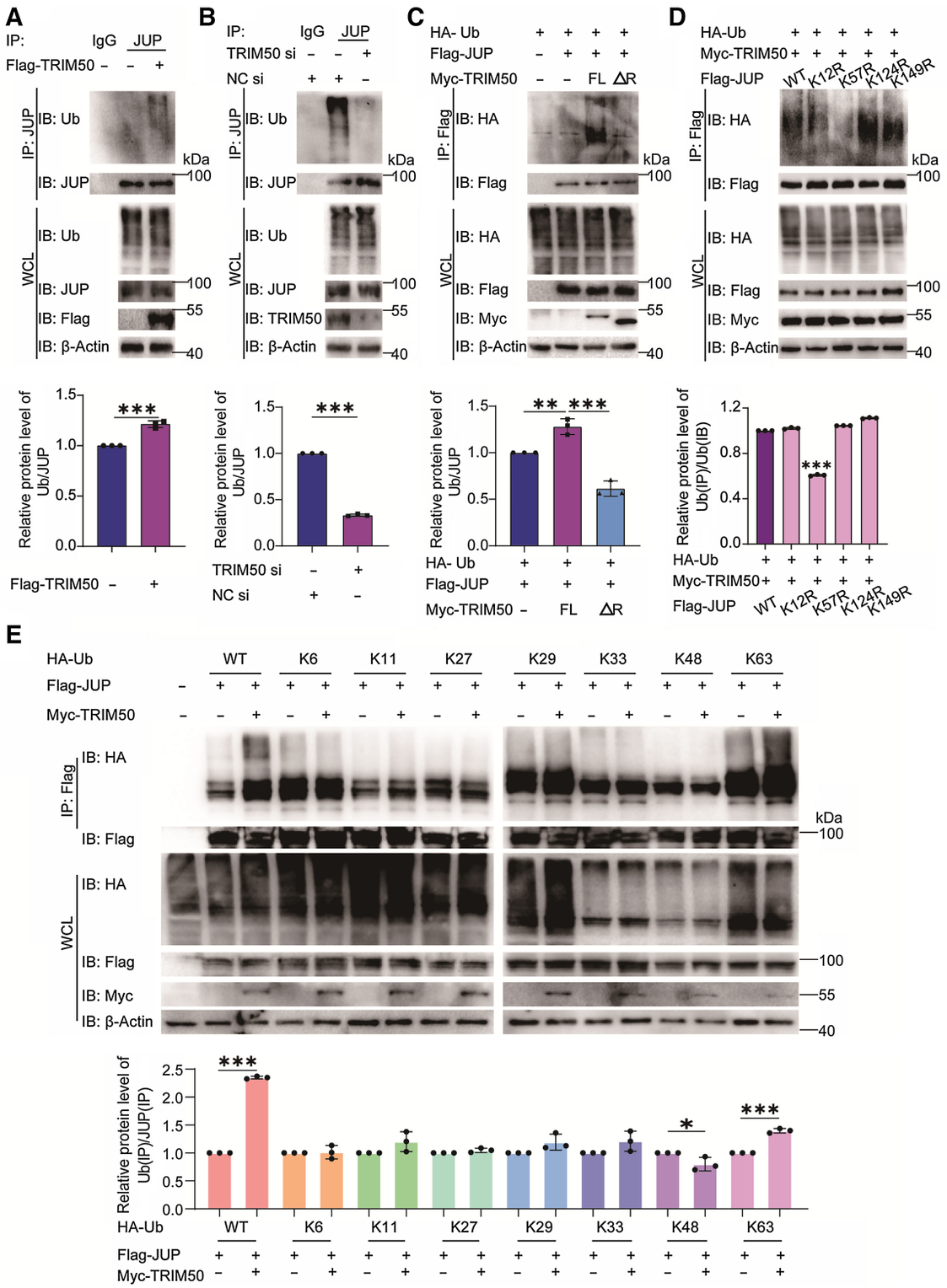

Figure 6.

TRIM50 stimulates the K63-linked polyubiquitination of JUP. **A,** MKN45 cells were transfected with or without Flag-TRIM50. The lysates were subjected to SDS denaturation, immunoprecipitation with JUP antibody and immunoblot analysis with the indicated antibodies. **B,** SNU-668 cells were transfected with TRIM50 siRNA or NC siRNA. Whole-cell lysates were subjected to SDS denaturation, immunoprecipitation with JUP antibody and immunoblot analysis with the indicated antibodies. (*Continued on the following page.*)

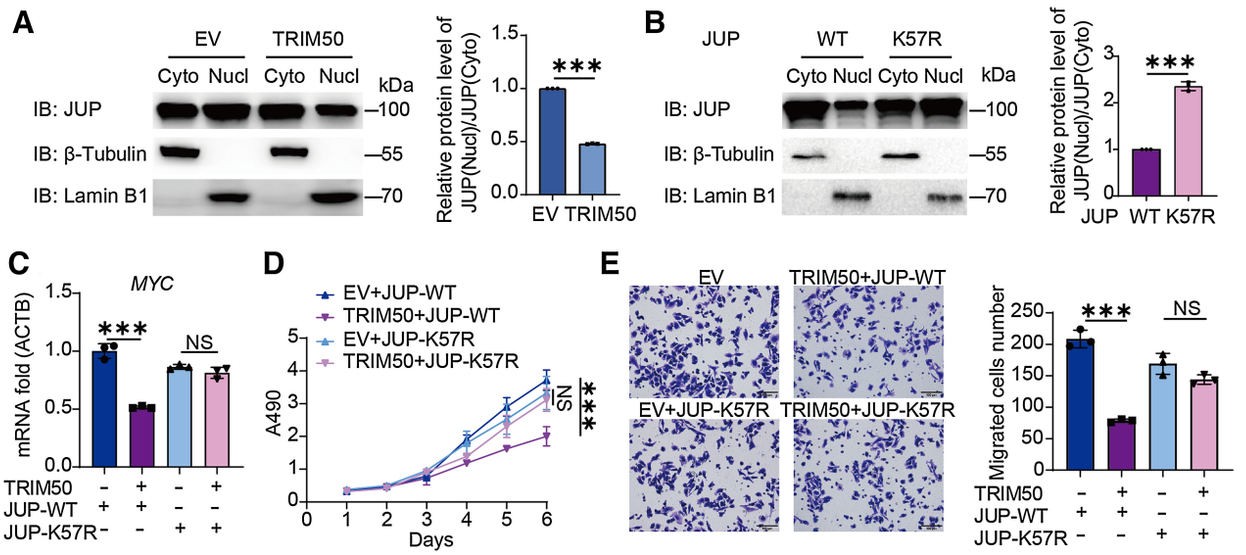

Figure 7.
TRIM50 inhibits the MYC signaling pathway in a JUP-dependent manner. **A,** Immunoblotting assay of the subcellular expression levels of JUP in TRIM50-overexpressing MKN45 cells. **B,** Immunoblotting assay of the subcellular expression levels of JUP in JUP (WT or K57R mutation)-overexpressing SNU-668 cells. **C,** RT-qPCR analysis of MYC in HGC27 cells. The cells were transfected with control plasmid or TRIM50 plasmid in combination with JUP (WT or K57R mutation) expression plasmid. **D,** Proliferation curve for HGC27 cells transfected with control plasmid or TRIM50 plasmid in combination with JUP (WT or the K57R mutant) expression plasmid. **E,** Images and quantification of Transwell migration assays with HGC27 cells transfected with control plasmid or TRIM50 plasmid in combination with JUP (WT or the K57R mutant) expression plasmid. Scale bar, 100 μm.

the nuclear localization sequence. Further experiments showed that compared to the WT protein, the JUP K57R mutant was more likely to accumulate in the nucleus in SNU-668 cells (**Fig. 7B**). JUP is expressed at low levels in HGC27 cells. We then transfected JUP WT or K57R mutant plasmids with the control or TRIM50 plasmid into HGC27 cells. Further analysis showed that unlike cells expressing WT JUP, TRIM50 overexpression failed to attenuate MYC gene expression in JUP K57R mutant-expressing HGC27 cells (**Fig. 7C**). Consistently, MTT and Transwell assays showed that TRIM50 overexpression did not significantly inhibit cell growth or migration in JUP K57R mutant-expressing HGC27 cells (**Fig. 7D** and **E**). These data indicated that TRIM50 regulates JUP nuclear transport in a ubiquitination-dependent manner.

Conclusion

In summary, our study showed that TRIM50 expression was downregulated in gastric cancer tissues compared with adjacent normal tissues and that a decrease in TRIM50 expression inhibited gastric cancer progression. TRIM50 restrained the activation of MYC signaling in gastric cancer by ubiquitylating JUP and inhibiting its nuclear translocation. Our study has revealed that TRIM50, a negative regulator of MYC, can inhibit gastric cancer progression, and TRIM50 has been shown to regulate JUP nuclear translocation, suggesting new therapeutic strategies for human malignancies with abnormal JUP accumulation.

Discussion

The regulatory effect of Ub-related enzymes on tumor progression is a research hotspot. In this study, we identified TRIM50 as one of the most dysregulated ubiquitination-related genes in gastric cancer by analyzing 814 ubiquitination-related genes in a GEO gastric cancer cohort. Subsequent experiments showed that TRIM50 suppressed gastric cancer growth and dissemination *in vitro* and *in vivo*. Furthermore, we identified JUP as a novel binding partner of TRIM50 in gastric cancer cells. Mechanistically, we first showed that TRIM50 increased the K63-linked ubiquitination of JUP and restrained its nucleocytoplasmic shuttling. This TRIM50-mediated reduction in nuclear JUP decreased MYC transcription and thus suppressed gastric cancer progression. Altogether, our findings have potential clinical implications for the treatment of gastric cancer by targeting the TRIM50/JUP/MYC axis.

TRIM family proteins, a subfamily of RING-type E3 Ub ligases, have been reported to regulate the progression of various cancer types, including gastric cancer. For example, TRIM44 promotes the EMT of cancer cells via the AKT/mTOR pathway in esophageal cancer (36).

(*Continued.*) **C,** 293T cells were transfected with HA-Ub, Flag-JUP along with Myc-empty vector (EV), Myc-TRIM50 full length (FL), and ΔR. Whole-cell lysates were subjected to immunoprecipitation with anti-Flag beads, and immunoblot analysis was performed. **D,** 293T cells were transfected with HA-Ub, Myc-TRIM50 along with Flag-empty vector (EV), Flag-JUP wild-type (WT), and mutant. Whole-cell lysates were subjected to immunoprecipitation with anti-Flag beads, and immunoblot analysis was performed. **E,** 293T cells were transfected with vectors expressing HA-Ub (WT, K6, K11, K27, K29, K33, K48 or K63) and plasmids encoding either Flag-JUP or Myc-TRIM50 alone or in combination. Whole-cell lysates were subjected to immunoprecipitation with anti-Flag beads, and immunoblot analysis was performed.

Knockdown of TRIM66 suppressed EMT and exhibited antitumor activity by inhibiting the JAK2/STAT3 signaling pathway in colorectal cancer (28). In addition, TRIM19, TRIM24, TRIM25 (also known as EFP), and TRIM68 govern the activation of nuclear receptors such as RAR and hormone receptors and have been linked to the development of leukemia (37). In gastric cancer, some TRIM family members also play important roles in cancer progression. TRIM32 and TRIM11 promote gastric cancer cell proliferation and invasion by activating β-catenin signaling (38, 39). TRIM54 promotes gastric cancer progression by upregulating K63 ubiquitination of filamin C, and high methylation levels were highly associated with a poor prognosis in patients with gastric cancer (40–42). In addition, TRIM59 promotes gastric carcinogenesis by promoting p53 ubiquitination and degradation (43). In our research, we found that TRIM50, another TRIM family member, is one of the most dysregulated ubiquitination-related genes in gastric cancer. First, we screened ubiquitination-related genes with significantly differential expression between gastric cancer tissues and adjacent tissues in the GSE66229 dataset. Furthermore, changes in TRIM50 mRNA and protein levels were validated with our gastric cancer samples and in other published datasets. TRIM50 was shown to be specifically expressed in gastric parietal cells and to control vesicular trafficking for acid secretion (22), suggesting that the downregulation of TRIM50 might result in altered gastric acid secretion and change the microbial environment, which may increase the risk of gastric cancer.

Unlike the tumor-promoting properties of most TRIM family members, TRIM50 acts as a tumor suppressor. It was reported that TRIM50 suppresses tumor growth in hepatocarcinoma and pancreatic cancer (19, 20). Moreover, TRIM50 reduces the progression of ovarian cancer (21). We constructed TRIM50-overexpressing MKN45 cells and performed a series of functional experiments demonstrating that TRIM50 overexpression can promote gastric cancer progression. MKN74 is less tumorigenic than MKN45, and more cells were used in the subcutaneous tumorigenesis assay. Knockdown of TRIM50 promoted gastric cancer progression, as expected.

MYC is an influential cancer driver that is excessively activated in a wide range of human malignancies. MYC activation occurs in tumor cells via several mechanisms, such as mutations in signaling pathway proteins upstream of MYC or direct modification of the MYC gene (44). JUP, also named plakoglobin or γ-catenin, is a nonclassical Wnt signaling pathway protein that can strongly activate c-Myc expression via Tcf/Lef-dependent mechanisms (26). In our study, TRIM50 inhibited the MYC pathway partially through JUP.

JUP participates in cell signaling, like its homolog β-catenin, in addition to its classic function in cell–cell adhesion (45). Several studies have suggested the oncogenic activity of JUP (46–49). Chen and colleagues revealed that the biofunctions of JUP in gastric carcinoma depend on its subcellular localization. Membrane and cytoplasm JUP restrain AKT/GSK3β/β-catenin signaling activity, whereas nuclear JUP collaborates with β-catenin to promote gastric cancer cell invasion (35). However, the regulatory mechanism of JUP subcellular localization has not been reported. In our work, we performed co-IP and MS in gastric cancer cells and revealed JUP as a novel target of TRIM50. We found that TRIM50 targets the JUP K57 site for K63-linked ubiquitination and thus restrains its nuclear translocation. JUP can directly activate c-myc expression in a Tcf/Lef-dependent manner. Therefore, we examined activation of the Tcf/Lef canonical Wnt/β-catenin pathway upon TRIM50 expression by TOPFLASH assay. We found that TRIM50 expression-associated cytoplasmic retention of JUP could inhibit the transcriptional activity of Tcf/Lef (Supplementary Fig. S7; Supplementary Information). It was previously reported that K63-linked polyubiquitination regulates the cytoplasmic localization of the target protein dystrophy type 1 (DM1) in the brain (50). Because the subcellular distribution of JUP is closely related to gastric cancer development and tumor differentiation status, changing JUP nuclear and membrane/cytoplasm expression by modulating its ubiquitination is expected to be a new strategy for cancer therapy.

In summary, our study shows that low expression levels of TRIM50 are positively correlated with malignant behaviors in gastric cancer. TRIM50 suppresses gastric cancer progression by interacting with JUP to promote its ubiquitination and nuclear translocation. Our findings showing that TRIM50 can inhibit JUP nucleocytoplasmic shuttling will provide new therapeutic strategies for human malignancies with abnormal accumulation of nuclear JUP.

Authors' Disclosures

No disclosures were reported.

Authors' Contributions

J. Hu: Conceptualization, resources, data curation, writing–original draft, writing–review and editing. **R. Huang:** Software, formal analysis. **C. Liang:** Data curation, software. **Y. Wang:** Supervision, writing–review and editing. **M. Wang:** Resources, validation. **Y. Chen:** Software, formal analysis. **C. Wu:** Validation, investigation. **J. Zhang:** Validation, investigation. **Z. Liu:** Software, formal analysis. **Q. Zhao:** Data curation, software, formal analysis. **Z. Liu:** Resources, methodology. **F. Wang:** Supervision, funding acquisition, project administration, writing–review and editing. **S. Yuan:** Conceptualization, project administration, writing–review and editing.

Acknowledgments

This work was supported in part by the International Cooperation and Exchanges National Natural Science Foundation of China (82061160373), National Natural Science Foundation of China (81872011), Science and Technology Program of Guangzhou (202206080011), and Sun Yat-sen University Clinical Research 5010 Program (2018014).

The publication costs of this article were defrayed in part by the payment of publication fees. Therefore, and solely to indicate this fact, this article is hereby marked "advertisement" in accordance with 18 USC section 1734.

Note

Supplementary data for this article are available at Molecular Cancer Research Online (http://mcr.aacrjournals.org/).

Received February 24, 2023; revised May 4, 2023; accepted June 28, 2023; published first July 6, 2023.

References

1. Sung H, Ferlay J, Siegel RL, Laversanne M, Soerjomataram I, Jemal A, et al. Global cancer statistics 2020: GLOBOCAN estimates of incidence and mortality worldwide for 36 cancers in 185 countries. CA Cancer J Clin 2021;71:209–49.
2. Colquhoun A, Arnold M, Ferlay J, Goodman KJ, Forman D, Soerjomataram I, et al. Global patterns of cardia and non-cardia gastric cancer incidence in 2012. Gut 2015;64:1881–8.
3. Plummer M, Franceschi S, Vignat J, Forman D, de Martel C. Global burden of gastric cancer attributable to Helicobacter pylori. Int J Cancer 2015;136:487–90.
4. Zhang HJ, Liu W, Bai X. [Influence of psychological factors on the quality of life of patients with non-surgical gastric cancer]. Zhongguo Yi Xue Ke Xue Yuan Xue Bao. Acta Academiae Medicinae Sinicae 2022;44:600–5.

5. Bray F, Ferlay J, Soerjomataram I, Siegel RL, Torre LA, Jemal A, et al. Global cancer statistics 2018: GLOBOCAN estimates of incidence and mortality worldwide for 36 cancers in 185 countries. CA Cancer J Clin 2018;68:394–424.
6. Smyth EC, Nilsson M, Grabsch HI, van Grieken NC, Lordick F. Gastric Cancer Lancet 2020;396:635–48.
7. Joshi SS, Badgwell BD. Current treatment and recent progress in gastric cancer. CA Cancer J Clin 2021;71:264–79.
8. Zeng Y, Jin RU. Molecular pathogenesis, targeted therapies, and future perspectives for gastric cancer. Semin Cancer Biol 2022;86(Pt 3):566–82.
9. Rape M. Ubiquitylation at the crossroads of development and disease. Nat Rev Mol Cell Biol 2018;19:59–70.
10. Tanaka K, Suzuki T, Chiba T. The ligation systems for ubiquitin and ubiquitin-like proteins. Mol Cells 1998;8:503–12.
11. Han S, Wang R, Zhang Y, Li X, Gan Y, Gao F, et al. The role of ubiquitination and deubiquitination in tumor invasion and metastasis. Int J Biol Sci 2022;18:2292–303.
12. Lee PCW, Dodart J-C, Aron L, Finley LW, Bronson RT, Haigis MC, et al. Altered social behavior and neuronal development in mice lacking the Uba6-Use1 ubiquitin transfer system. Mol Cell 2013;50:172–84.
13. Urbán N, van den Berg DLC, Forget A, Andersen J, Demmers JAA, Hunt C, et al. Return to quiescence of mouse neural stem cells by degradation of a proactivation protein. Science 2016;353:292–5.
14. Werner A, Iwasaki S, McGourty CA, Medina-Ruiz S, Teerikorpi N, Fedrigo I, et al. Cell-fate determination by ubiquitin-dependent regulation of translation. Nature 2015;525:523–7.
15. Hoeller D, Dikic I. Targeting the ubiquitin system in cancer therapy. Nature 2009;458:438–44.
16. Li D, Wang Y, Dong C, Chen T, Dong A, Ren J, et al. CST1 inhibits ferroptosis and promotes gastric cancer metastasis by regulating GPX4 protein stability via OTUB1. Oncogene 2023;42:83–98.
17. Wang Z, Kang W, Li O, Qi F, Wang J, You Y, et al. Abrogation of USP7 is an alternative strategy to downregulate PD-L1 and sensitize gastric cancer cells to T cells killing. Acta Pharm Sin B 2021;11:694–707.
18. Hatakeyama S. TRIM family proteins: roles in autophagy, immunity, and carcinogenesis. Trends Biochem Sci 2017;42:297–311.
19. Li R, Zhu L, Peng Y, Zhang X, Dai C, Liu D. TRIM50 suppresses pancreatic cancer progression and reverses the epithelial-mesenchymal transition via facilitating the ubiquitous degradation of snail1. Front Oncol 2021;11:695740.
20. Ma X, Ma X, Qiu Y, Zhu L, Lin Y, You Y, et al. TRIM50 suppressed hepatocarcinoma progression through directly targeting SNAIL for ubiquitous degradation. Cell Death Dis 2018;9:608.
21. Qiu Y, Liu P, Ma X, Ma X, Zhu L, Lin Y, et al. TRIM50 acts as a novel Src suppressor and inhibits ovarian cancer progression. Biochim Biophys Acta Mol Cell Res 2019;1866:1412–20.
22. Nishi M, Aoyama F, Kisa F, Zhu H, Sun M, Lin P, et al. TRIM50 protein regulates vesicular trafficking for acid secretion in gastric parietal cells. J Biol Chem 2012;287:33523–32.
23. ten Have S, Boulon S, Ahmad Y, Lamond AI. Mass spectrometry-based immunoprecipitation proteomics - the user's guide. Proteomics 2011;11:1153–9.
24. Yashiro M, Chung YS, Nishimura S, Inoue T, Sowa M. Peritoneal metastatic model for human scirrhous gastric carcinoma in nude mice. Clin Exp Metastasis 1996;14:43–54.
25. Smith BN, Bhowmick NA. Role of EMT in metastasis and therapy resistance. J Clin Med 2016;5:17.
26. Barker N, Clevers H. Catenins, Wnt signaling and cancer. Bioessays 2000;22:961–5.
27. Müller-Tidow C, Steffen B, Cauvet T, Tickenbrock L, Ji P, Diederichs S, et al. Translocation products in acute myeloid leukemia activate the Wnt signaling pathway in hematopoietic cells. Mol Cell Biol 2004;24:2890–904.
28. Luong-Gardiol N, Siddiqui I, Pizzitola I, Jeevan-Raj B, Charmoy M, Huang Y, et al. γ-Catenin-dependent signals maintain BCR-ABL1(+) B cell acute lymphoblastic leukemia. Cancer Cell 2019;35:649–63.
29. Short KM, Cox TC. Subclassification of the RBCC/TRIM superfamily reveals a novel motif necessary for microtubule binding. J Biol Chem 2006;281:8970–80.
30. Zhou X, Zheng W, Li Y, Pearce R, Zhang C, Bell EW, et al. I-TASSER-MTD: a deep-learning-based platform for multi-domain protein structure and function prediction. Nat Protoc 2022;17:2326–53.
31. Swatek KN, Komander D. Ubiquitin modifications. Cell Res 2016;26:399–422.
32. Hershko A, Ciechanover A. The ubiquitin system. Annu Rev Biochem 1998;67:425–79.
33. Chen ZJ& Sun LJ. Nonproteolytic functions of ubiquitin in cell signaling. Mol Cell 2009;33:275–86.
34. Venuto S, Merla G. E3 ubiquitin ligase TRIM proteins, cell cycle and mitosis. Cells 2019;8:510.
35. Chen Y, Yang L, Qin Y, Liu S, Qiao Y, Wan X, et al. Effects of differential distributed-JUP on the malignancy of gastric cancer. J Adv Res 2021;28:195–208.
36. Xiong D, Jin C, Ye X, Qiu B, Jianjun X, Zhu S, et al. TRIM44 promotes human esophageal cancer progression via the AKT/mTOR pathway. Cancer Sci 2018;109:3080–92.
37. Hatakeyama S. TRIM proteins and cancer. Nat Rev Cancer 2011;11:792–804.
38. Lan Q, Tan X, He P, Li W, Tian S, Dong W. TRIM11 promotes proliferation, migration, invasion and EMT of gastric cancer by activating beta-catenin signaling. Onco Targets Ther 2021;14:1429–40.
39. Wang C, Xu J, Fu H, Zhang Y, Zhang X, Yang D, et al. TRIM32 promotes cell proliferation and invasion by activating beta-catenin signalling in gastric cancer. J Cell Mol Med 2018;22:5020–8.
40. Cao H, Li Y, Chen L, Lu Z, You T, Wang X, et al. Tripartite motif-containing 54 promotes gastric cancer progression by upregulating K63-linked ubiquitination of filamin C. Asia Pac J Clin Oncol 2022;18:669–77.
41. Nakajima T, Maekita T, Oda I, Gotoda T, Yamamoto S, Umemura S, et al. Higher methylation levels in gastric mucosae significantly correlate with higher risk of gastric cancers. Cancer Epidemiol Biomarkers Prev 2006;15:2317–21.
42. Shi J, Zhang G, Yao D, Liu W, Wang N, Ji M, et al. Prognostic significance of aberrant gene methylation in gastric cancer. Am J Cancer Res 2012;2:116–29.
43. Zhou Z, Ji Z, Wang Y, Li J, Cao H, Zhu HH, et al. TRIM59 is up-regulated in gastric tumors, promoting ubiquitination and degradation of p53. Gastroenterology 2014;147:1043–54.
44. Anauate AC, Leal MF, Calcagno DQ, Gigek CO, Karia BTR, Wisnieski F, et al. The complex network between MYC oncogene and microRNAs in gastric cancer: an overview. Int J Mol Sci 2020;21:1782.
45. Pasdar M, Li Z, Chlumecky V. Plakoglobin: kinetics of synthesis, phosphorylation, stability, and interactions with desmoglein and E-cadherin. Cell Motil Cytoskeleton 1995;32:258–72.
46. Kolligs FT, Kolligs B, Hajra KM, Hu G, Tani M, Cho KR, et al. gamma-catenin is regulated by the APC tumor suppressor and its oncogenic activity is distinct from that of beta-catenin. Genes Dev 2000;14:1319–31.
47. Bommer GT, Jäger C, Dürr E-M, Baehs S, Eichhorst ST, Brabletz T, et al. DRO1, a gene down-regulated by oncogenes, mediates growth inhibition in colon and pancreatic cancer cells. J Biol Chem 2005;280:7962–75.
48. Pan H, Gao F, Papageorgis P, Abdolmaleky HM, Faller DV, Thiagalingam S. Aberrant activation of gamma-catenin promotes genomic instability and oncogenic effects during tumor progression. Cancer Biol Ther 2007;6:1638–43.
49. Morin PJ, Sparks AB, Korinek V, Barker N, Clevers H, Vogelstein B, et al. Activation of beta-catenin-Tcf signaling in colon cancer by mutations in beta-catenin or APC. Science 1997;275:1787–90.
50. Wang PY, Chang KT, Lin YM, Kuo TY, Wang GS. Ubiquitination of MBNL1 is required for its cytoplasmic localization and function in promoting neurite outgrowth. Cell Rep 2018;22:2294–306.